Acclimation limits for embolism resistance and osmotic adjustment accompany the geographical dry edge of Mediterranean species

Asaf Alon, Shabtai Cohen, Régis Burlett, Uri Hochberg, Victor Lukyanov, Ido Rog, Tamir Klein, Hervé H. Cochard, Sylvain Delzon, Rakefet David-schwartz

Received: 17 August 2022 | Accepted: 25 January 2023

DOI: 10.1111/1365-2435.14289

Functional Ecology | BRITISH ECOLOGICAL SOCIETY

RESEARCH ARTICLE

Acclimation limits for embolism resistance and osmotic adjustment accompany the geographical dry edge of Mediterranean species

Asaf Alon[1,2,3] | Shabtai Cohen[2] | Régis Burlett[4] | Uri Hochberg[2] | Victor Lukyanov[2] | Ido Rog[5] | Tamir Klein[5] | Hervé Cochard[6] | Sylvain Delzon[4] | Rakefet David-Schwartz[1]

[1]Volcani Center, Agricultural Research Organization, Institute of Plant Sciences, Rishon LeZion, Israel; [2]Volcani Center, Agricultural Research Organization, Institute of Soil, Water and Environmental Sciences, Rishon LeZion, Israel; [3]The Robert H. Smith Faculty of Agriculture, Food and Environment, Institute of Plant Sciences and Genetics in Agriculture, The Hebrew University of Jerusalem, Rehovot, Israel; [4]University of Bordeaux, INRAE, BIOGECO, Pessac, France; [5]Department of Plant and Environmental Sciences, Weizmann Institute of Science, Rehovot, Israel and [6]Université Clermont Auvergne, INRAE, PIAF, Clermont-Ferrand, France

Correspondence
Rakefet David-Schwartz
Email: rakefetd@volcani.agri.gov.il

Funding information
The Ministère des Affaires Etrangères et du Développement International (France) and the Ministry of Science (Israel), Grant/Award Number: Maïmonide-Israel

Handling Editor: Katie Field

Abstract

- Survival and growth of woody species in the Mediterranean are mainly restricted by water availability. We tested the hypothesis that Mediterranean species acclimate their xylem vulnerability and osmotic potential along a precipitation gradient.
- We studied five predominant co-occurring Mediterranean species; *Quercus calliprinos*, *Pistacia palaestina*, *Pistacia lentiscus*, *Rhamnus lycioides* and *Phillyrea latifolia*, over two summers at three sites. The driest of the sites is the distribution edge for all the five species. We measured key hydraulic and osmotic traits related to drought resistance, including resistance to embolism (Ψ_{50}) and the seasonal dynamics of water and osmotic potentials.
- The leaf water potentials (Ψ_l) of all species declined significantly along the summer, reaching significantly lower Ψ_l at the end of summer in the drier sites. Surprisingly, we did not find plasticity along the drought gradient in Ψ_{50} or osmotic potentials. This resulted in much narrower hydraulic safety margins (HSMs) in the drier sites, where some species experienced significant embolism.
- Our analysis indicates that reduction in HSM to null values put Mediterranean species in embolism risk as they approach their hydraulic limit near the geographical dry edge of their distribution.

KEYWORDS
climate change, drought resistance, hydraulic failure, hydraulic safety margins, osmotic adjustment, tree hydraulics

1 | INTRODUCTION

Drought is projected to increase in intensity and duration in many regions world-wide, including the Mediterranean (Spinoni et al., 2018; Xu et al., 2019), a hot spot for biodiversity (Myers et al., 2000). The current massive tree mortality in parts of the region is a major cause of concern for the extinction of native species (Cramer et al., 2018; García de la Serrana et al., 2015). Deciphering drought-resistance strategies and their limitations in Mediterranean woody species is crucial for understanding changes in structure and function of plant communities threatened by climate change and will help improve forests and woodlands' sustainable management programs (Trumbore et al., 2015).

The various strategies used by woody species to cope with drought stress can be divided into three categories; escape, avoidance and tolerance (Delzon, 2015; Volaire, 2018). Escape is the temporary shedding of leaves and branches through which water is lost. Avoidance actively minimizes water loss by stomatal closure or increasing water uptake through deep roots. Tolerance maintains physiological functionality during water loss, mainly by increased xylem resistance to embolism and osmotic adjustment to prevent turgor loss at the cell level. Woody species vary in their strategies to cope with drought, especially under natural conditions of prolonged and severe drought. Therefore, field studies of natural populations for a wide range of species and traits and along aridity gradients are necessary.

Drought can lead to embolism, a process that occurs via cavitation events in the xylem and causes hydraulic dysfunction by disrupting water conduction in the xylem (Tyree & Zimmermann, 1983). Embolism resistance is often expressed as the value of xylem water potential (Ψ_x) corresponding to 50 or 88 % loss of conductivity (PLC), Ψ_{50} and Ψ_{88} respectively (Tyree & Sperry, 1989). Embolism has been shown to be highly associated with tree mortality worldwide (Adams et al., 2017; Anderegg et al., 2016). The variation in embolism resistance between species is large, and it appears that species habitat dryness plays a substantial role in this variation (Choat et al., 2012; Delzon et al., 2010; Larter et al., 2017; Maherali et al., 2004; Skelton et al., 2018). As opposed to the large interspecific variation, it seems that intraspecific variation in resistance to embolism is limited. However, an analysis of 46 species suggests that significant intraspecific variation may occur (Anderegg, 2015).

Leaf water potential (Ψ_l) is an indicator of plant water status. Predawn leaf Ψ (Ψ_{PD}) is measured when the plant is in equilibrium with soil water and is a measure of the soil water availability as perceived by the plant. Ψ_{PD} is affected by drought severity and root depth (Nardini et al., 2016). The difference between either the Ψ_{12}, Ψ_{50} or Ψ_{88} value and the minimum water potential observed in field conditions (Ψ_{min}) is defined as the hydraulic safety margins (HSMs, Martin-StPaul et al., 2017; Meinzer et al., 2009). In order to keep wide HSMs, plants use their ability to minimize stomatal aperture, that is, a plastic response. A narrow HSM means proximity to thresholds with a risk of hydraulic failure. A meta-analysis showed that most plants that resist drought do so by stomatal closure at a much higher water potential than that which causes hydraulic failure (Martin-StPaul et al., 2017), suggesting that species in nature avoid hydraulic failure by sacrificing photosynthesis (Creek et al., 2020; Johnson et al., 2011; Martin-StPaul et al., 2017; Meinzer et al., 2009).

Stomatal closure has been shown to be correlated with the cell turgor loss point (TLP, Bartlett et al., 2016; Martin-StPaul et al., 2017; Mencuccini et al., 2015). Plants may invest energy to reduce the cell TLP during dehydration to keep cells turgid. The water potential for TLP (Ψ_{TLP}) can be reduced through increasing cell wall elasticity (reduced modulus of elasticity, ε; i.e. elastic adjustment), increasing the extracellular water content (increasing a_f; i.e. apoplastic adjustment) and active accumulation of solutes (decreasing osmotic potential at full turgor, Π_0; i.e. osmotic adjustment, Bartlett et al., 2012; Meinzer et al., 2014). While Π_0 was found to reveal the plasticity of osmotic adjustment related to environmental changes in many species (Bartlett et al., 2012), evidence for a correlation of ε with response to drought is limited (Meinzer et al., 2014).

Studies focusing on leaf traits of coexisting woody species in Mediterranean climates reveal variation in response to drought during the long rainless summer. In response to extreme drought, leaf defoliation was observed in *Juniperus phoenicea*, *Rosmarinus officinalis* and *Rhamnus lycioides* but not in four other coexisting species (Gazol et al., 2017). Dehydration avoidance via stomatal closure at the cost of low carbon assimilation was demonstrated by *Pinus nigra*, while neighbouring *Quercus ilex* and *Quercus faginea* showed dehydration tolerance via osmotic adjustment. The observed osmotic adjustment was more robust in the evergreen *Q. ilex* than in the semideciduous *Q. faginea*, explaining its better resistance to drought (Forner, Valladares, & Aranda, 2018). However, *Q. faginea* responded to intensified drought conditions with a more robust plastic stomatal response than *Q. ilex* (Forner, Valladares, Bonal, et al., 2018; Klein et al., 2013). Combined analysis of Ψ_{PD} and sap flow of five species allowed designating *Pinus halepensis*, *Pistacia lentiscus* and *Erica multiflora* as water savers versus *Quercus coccifera* and *Stipa tenacissima* as water spenders (Chirino et al., 2011).

The above studies imply interspecific differences in the plastic stomatal response or osmotic adjustment; however, resistance to embolism, a key trait in species resistance to drought, was missing from those studies. Pratt et al. (2007, 2012) found a large variation in resistance to embolism in Mediterranean climates among 19 fynbos species in South Africa and nine chaparral species of the Rhamnaceae in California. In a study conducting year-round measurements of resistance to embolism, water potential and Ψ_{TLP} in three coexisting species (Väänänen et al., 2020), it was found that *Phillyrea latifolia* tolerates drought via xylem resistance to embolism and osmotic adjustment, while coexisting *Pistacia lentiscus* and *Quercus calliprinos* avoid drought via stomatal regulation. However, these results did not explain the high mortality rate of *Q. calliprinos* compared to the other species, suggesting that an additional mechanism might occur in these coexisting species. This emphasizes the importance of evaluating a range of traits, species and aridity gradients to better represent each species' total traits repertoire used for drought resistance. Here, we tested the hypothesis that the hydraulic safety margins

(HSMs) of co-occurring species are preserved along an aridity gradient due to one or more of the plastic responses to drought, including resistance to embolism, stomatal closure and osmotic adjustment.

2 | MATERIALS AND METHODS

2.1 | Sites and species

The steep climatic gradient in Israel is governed by Mediterranean weather patterns, characterized by long, dry summers and changes gradually from mesic Mediterranean to arid from north to south (Tielbörger et al., 2014). Three sites were chosen to represent mesic Mediterranean (MM), Mediterranean (M) and semi-arid (SA) climate conditions along the natural rainfall gradient (Table 1). The three sites were undisturbed for the last 40 years, and thus represent ecologically equilibrated environments. No licence or permit was needed to carry out the work. Climate data were taken from stations of the Israel Meteorological Service (IMS, ims.gov.il); station Michmanim for the MM site, station Ramat Hanadiv for the M site, and station Netiv HaLamed-Heh for the SA site. All sites were characterized by a prolonged summer–fall rainless dry period, from the end of April to October. Aridity indexes (mean annual precipitation divided by potential evapotranspiration) for the SA, M and MM sites are 0.27, 0.39 and 0.46 respectively. Site aridity was also reflected by differences in leaf carbon isotope ratio ($\delta^{13}C$), which was measured in mature healthy sunlit leaves collected at the end of the dry period (August 2018) with a ^{13}C cavity ring down analyser (G2131i, Picarro) as described by Nemera et al. (2020). Leaf intrinsic water-use efficiency (WUEi) was calculated using the species mean based on a leaf-scale model of C3 photosynthetic isotope discrimination (Farquhar et al., 1989):

$$WUI_i = \frac{C_a(b - \delta^{13}C)}{1.6(b - a)}, \quad (1)$$

Where C_a is the atmospheric CO_2 concentration in PPM and a and b are fractionation factors occurring during diffusion of CO_2 through stomata pores (4.4‰) and enzymatic carbon fixation by Rubisco plus a small component accounting for mesophyll conductance (27‰) respectively.

Lower leaf $\delta^{13}C$ in leaves that grew during the dry season at the more humid sites indicates that internal [CO_2] was higher there during photosynthesis, allowing more fractionation during carboxylation, which is indicative of more open stomata. Leaf $\delta^{13}C$ can also be taken a proxy for WUEi, which is the ratio between carbon assimilation and stomatal conductance (see Figure S1 in Supporting Information, Cernusak et al., 2013). The site influence on leaf $\delta^{13}C$ was significant in the two-factorial ANOVA (see Table S1). Annual precipitation (from September to August) in 2017–2018 was 700, 624 and 337 mm, and in 2018–2019 was 1039, 651 and 504 mm at the MM, M and SA sites respectively. The average daily maximum temperature in July was 30°C, 32°C and 31°C at the MM, M and SA sites respectively (Figure 1a). Maximum VPD in the summer was 2.5, 3 and 4 kPa for the MM, M and SA sites respectively (Figure 1b). Soil types varied between the sites and the degree of clayey soil decreased from north to south. Five predominant native woody species were selected for the research (Table 2), which coexisted in 2500 square metre plots at each of the three research sites. The SA site is close to the dry southern limit of the Mediterranean zone and the studied species (see Figure S2, Danin & Plitmann, 1987).

For all trait measurements described below, samples were taken from specific five labelled individuals per species at each site, unless otherwise stated.

2.2 | Hydraulic vulnerability measurements

Vulnerability curves (VCs) for per cent loss of conductivity (PLC) of stem samples as a function of water potential were measured in a Cavitron (Cochard et al., 2005). We have shown that different methods for PLC measurement can give significantly different PLC values, and therefore it is important to use the same method when doing comparative studies (David-Schwartz et al., 2016). In the current study, Cavitron measurements were done for all species except QC, which was not measured due to its long vessels (>30 cm, personal data). In addition, due to the growth characteristics at the study sites, it was impossible to find strait QC branches of 1 m long for measurements in a nonstandard Cavitron with a large rotor diameter. Thus, we measured the PLC values of *Quercus coccifera*, which is an evergreen oak that belongs to the subgenus *Quercus* section *Cerris* and is considered a subspecies of QC (Toumi & Lumaret, 2010). Two branches from three *Q. coccifera*

TABLE 1 Three selected sites with main geographical, edaphic and climatic characteristics.

Code site	AI[a]	Latitude	Longitude	Elevation (m)	MAP[a] (mm)	SMT[a] (°C)	WMT[a] (°C)	Soil type[b]
MM	0.46	32°54′N	35°20′E	430	700	30	10	TR
M	0.39	32°33′N	34°56′E	80	550	32	16	TR and R
SA	0.27	31°40′N	34°56′E	300	400	31	17	Bright and Brown R

[a]AI, Aridity index is the ratio of the annual precipitation and potential evapotranspiration. MAP, mean annual precipitation; SMT, Average maximum daily temperature in July; WMT, Average maximum daily temperature in January. Data for 1981–2000, provided by the Israel Meteorological Service.
[b]Data taken from GIS site of Israel Agriculture office (https://moag.maps.arcgis.com/), TR and R correspond to Terra Rossa and Rendzinza respectively.

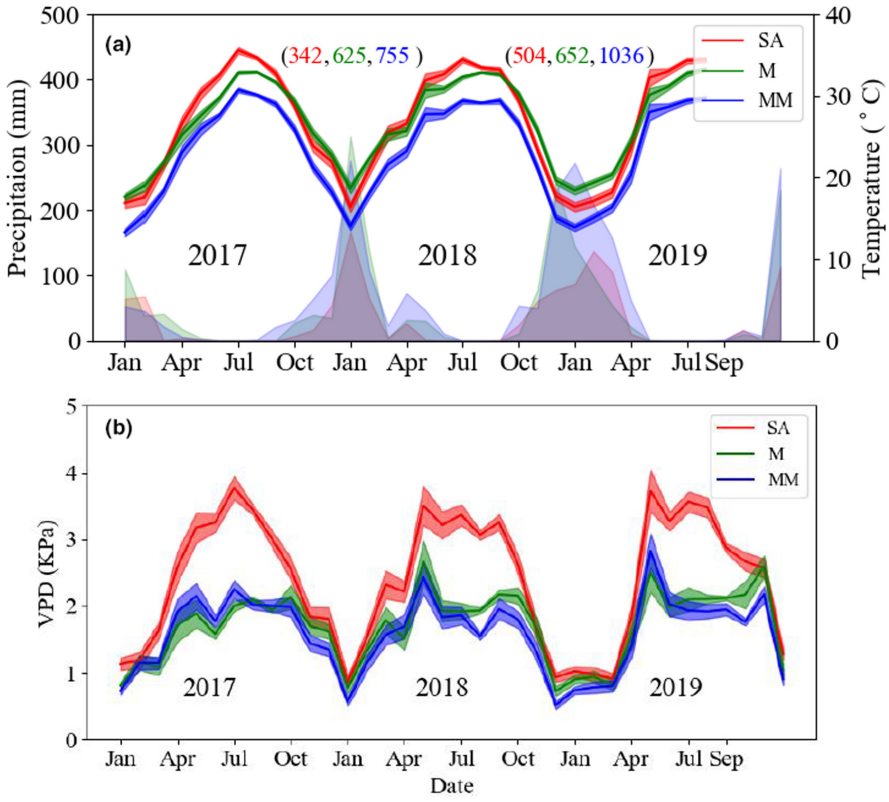

FIGURE 1 Meteorological data from the three study sites. (a) Monthly average daily maximum temperature (line chart) and monthly precipitation (area chart). Numbers in brackets represent the cumulative precipitation for two consecutive winters (2017–2018 and 2018–2019, calculated from September to September) for the SA (red), M (green) and MM (blue) sites respectively. (b) Monthly average daily maximum vapour pressure deficit (VPD). Line shadow represents standard error.

TABLE 2 Characteristics of species selected for the research.

Species	Code	Family	Life-form	Leaf phenology
Quercus calliprinos	QC	Fagaceae	Tree	Evergreen
Pistacia palaestina	PP	Anacardiaceae	Shrub/ Tree	Winter deciduous
Pistacia lentiscus	PL	Anacardiaceae	Shrub	Evergreen
Rhamnus lycioides	RL	Rhamnaceae	Shrub	Partially drought deciduous
Phillyrea latifolia	PHL	Oleaceae	Shrub	Evergreen

individuals collected from a site near Avignon (French Mediterranean basin) were used for the PLC measurements.

To avoid native embolism in branches that were tested for VC and PLC, samples were collected from the three sites at the end of the rainy season (April 2018), when water potentials were less negative than −1.5 MPa. Samples of RL at the MM site were not included in this analysis, as its branches were too short for the Cavitron. Two terminal branches (1 cm diameter and 100 cm in length) were harvested from the upper canopy of five to seven individuals of each species and were sent in overnight mail to France (to Bordeaux and Clermont-Ferrand). VCs were determined as previously described (Lamy et al., 2014). PLC was calculated every 1–2 MPa, following the equation:

$$\mathrm{PLC} = 100 * \left(1 - \frac{K}{K_{\max}}\right). \quad (2)$$

The sigmoidal curve was fitted to the following equation (Pammenter & Van der Willigen, 1998):

$$\mathrm{PLC} = \frac{100}{\left[1 + \exp\left(\frac{S}{25} * \left(\Psi - \Psi_{50}\right)\right)\right]}, \quad (3)$$

where Ψ_{50} (MPa) is the xylem pressure inducing 50% loss of conductance and S (% MPa^{-1}) is the slope of the vulnerability curve at the inflection point. Predicted PLC (PLC_p) was calculated according to the actual leaf water potential and Equation (2).

2.3 | Field measurements of water potential

Field campaigns were conducted monthly at all sites during the rainless period (May–September) in two consecutive years; 2018, where predawn and midday water potentials were measured (Ψ_{PD} and Ψ_{MD} respectively), and in 2019, where only Ψ_{MD} was measured. Twigs for Ψ_{PD} were taken at 4:30 am, while twigs for Ψ_{MD} were taken at 12:30 pm. The twigs were kept in sealed plastic bags in a dark cold container until measurements were taken after a couple of hours.

The measurements were made in a Scholander-type pressure chamber (PMS, Corvallis, OR, USA). The decline in Ψ_{MD} in relation to soil dehydration (as reflected by Ψ_{PD}) was analysed according to Meinzer et al. (2016). Regression lines were calculated for all species for each site. Slopes, hydroscapes (HS) (which is a metric of stomatal control based on the area between the 1:1 line and the regression slope) and Ψ_{g_0} (extrapolated to find the value at which $\Psi_{PD} = \Psi_{MD}$) were calculated from the above analysis both for different sites for each species and for each species separately at all sites included. Ψ_{min} was taken as the lowest value of measured midday water potential in the field. Hydraulic safety margins (HSMs) were calculated as $\Psi_{min} - \Psi_x$, where Ψ_x is the xylem pressure inducing 12, 50 or 88% loss of branch hydraulic conductivity.

2.4 | Osmotic potential

Seasonal change in osmotic potential was measured five times along the summer of 2019. For each leaf sample, both Ψ_{MD} and native osmotic potential (Ψ_s) were concurrently measured. For full turgor osmotic potential (Π_0) measurements, an additional shoot, harvested from each individual, was cut under water, rehydrated for 2 h, and measured in the pressure chamber to verify rehydration. For both cases (Ψ_s and Π_0), samples were packed into 250 μL tubes and were frozen in liquid nitrogen. Upon thawing, holes were drilled in the bottom of the frozen tubes, which were then put into other clean tubes that collected the liquid when centrifuged at 15000 RCF (g) for 2 min. Ten microlitres from each Osmolality (mmol) of the samples was assessed with a vapour pressure osmometer (VAPRO 5520 Wescor). Conversion to pressure units was done by Van't Hoff equation:

$$\Psi_\pi(\text{MPa}) = nRT / 10000, \quad (4)$$

in which n is the solute concentration in mol/L, R is the universal gas constant (8.314472 L bar K^{-1} mol^{-1}) and T is the temperature in °K. Temperature was taken as 25^0; conversion ratio was 403.33 mmol/MPa.

Ψ_s and Π_0 were analysed by correlation with the Ψ_{MD} values, and by covariance analyses which were performed to test the influence of Ψ_{MD}, site and the interaction between Ψ_{MD} and site on Ψ_s and Π_0. Slope regression analysis of Ψ_s versus Ψ_{MD} is a proxy for the osmotic potential due to both solute concentration (reduced cell volume) and osmotic adjustment (OA, i.e. active solute accumulation), while slope regression analysis of Π_0 versus Ψ_{MD} is a proxy for OA only (Turner, 2017, 2018).

2.5 | Species characterization by drought-resistance strategies

Tolerance, avoidance and escape were quantified as numbers between 0 and 1 (less to most respectively) for each species. Each strategy was evaluated from the below measured parameters which were converted to normalized values (NVs) as follows:

$$NV = (x - \text{min}) / (\text{max} - \text{min}), \quad (5)$$

where x is the measured value, and min and max are the minimum and maximum thresholds of each parameter, which are either based on the theoretical limit for the measured parameters as describes below or on known values from the literature.

'Tolerance' was calculated as the average of 'xylem tolerance' and 'osmoregulation'. Xylem tolerance was taken to be a normalized value of Ψ_{50}. Values for normalization were from 0 to −18 MPa, the latter being the most negative Ψ_{50} reported (Larter et al., 2015). 'Osmoregulation' was normalized from the slope of Ψ_{MD} versus Π_0. Values for normalization were from 0 to 1.

'Avoidance' was calculated as the average of 'water access' and 'Stringency of stomatal control'. 'Water access' was normalized from the minimum seasonal Ψ_{PD} at the SA site. Values for normalization were from 0 to −10 MPa. Normalized values were subtracted from 1. 'Stringency of stomatal control' was normalized from HS, calculated from Ψ_{PD} versus Ψ_{MD} according to Meinzer et al. (2016), where the full range of values was from 0 to 10 MPa. Normalized values were subtracted from 1.

'Escape' was the rank for 'Drought deciduous'. 'Drought deciduous' was evaluated from the literature (1, 0.5 and 0, refer to full-, partial- and nondeciduous respectively). Among the studied species, only RL is known to be partially drought deciduous (Gazol et al., 2017).

2.6 | Statistical analysis

One-way analysis of variance (ANOVA), Tukey–Kramer post hoc test and graphs plotting were done using Python software (Python Software Foundation, packages; SCIPY and STATSMODEL). Two-way ANOVA, analysis of covariance (ANCOVA) and Bartlett's test for homogeneity of variances were done using JMP 14 software (SAS Institute Inc.). Hydraulic traits were compared over species and sites by two-way ANOVA. In addition, comparisons of sites by species with regard to Ψ_{MD} and Ψ_S / Π_0 were performed by analysis of covariance with Ψ_{PD} and Ψ_{MD} as the covariate respectively. Comparison of species by site was done analogously. The Tukey–Kramer post hoc test was used to compare the results where applicable. In all cases, validity of ANOVA assumptions was tested using the model residuals. To test the hypothesis of equal variances in the relevant populations, we used the Bartlett's test for homogeneity of variances, which is used for three or more independent samples, where a sample variance can be calculated for each sample (Zar, 1984). Bartlett's test for homogeneity of variances was used to compare interspecific variation between means among sites and along the season within sites. The threshold for statistical significance was set at $p < 0.05$.

3 | RESULTS

3.1 | Effect of environmental drought on hydraulic traits

3.1.1 | Resistance to embolism

Large differences in resistance to embolism were found between species (Figure 2), with PHL demonstrated the most negative Ψ_{50} value (< −10 MPa) followed by RL and PL, while PP showed the least negative value (~ −5 MPa). PLC curves of all species are provided as Supporting Information Figure S3. All parameters of vulnerability curves for resistance to embolism per species, including slope, Ψ_{12}, Ψ_{50} and Ψ_{88}, were similar at the three sites (Figure 2, Table 3, Table S2), and were not influenced by the site, as shown by a two-factorial ANOVA (Table 3).

3.1.2 | Leaf water potential

In each sampling along the dry season, Ψ_{PD} values for each of the species were the lowest in the drier site as compared to the wetter sites (Figure 3, Table 3 and Table S3). Interspecific variations in water potential were evidenced at each site, and at each measurement event (see Tables S4 and S5). PHL had the most negative Ψ_{PD}, followed by RL and PL, while QC and PP had the highest Ψ_{PD} values (Figure 3a–e). The Ψ_{min} was determined as the Ψ_{MD} found at the end of the dry season at the SA site. Ψ_{min} was significantly lower with increasing site aridity in both 2018 and 2019 (Table 3, Figure 3f,g). Two-factorial ANOVA showed that Ψ_{min} was affected by the species and site, and was affected by the interaction of species-on-site only in 2018 (Table 3). For QC and PHL minimum values were close to, but did not decline below Ψ_{12}, while for the other species minimum Ψ_{MD} values were significantly lower than Ψ_{12} (Figure 3).

3.1.3 | HSM and PLCp

The HSM in 2018 was narrower at the SA site than at the M and MM sites for PL, PHL and RL, while QC and PP had narrower HSMs at the SA and M site in comparison to the MM site (Figure 4a,b, Table S2). These differences in HSM between the species were less prominent in 2019 (Figure 4d,e, Table S2), which was a wetter year (Table 3, Figure 1). Still, in both 2018 and 2019, HSM_{12} declined to negative values at the SA site for PP and RL (Figure 4a,d). These species demonstrated values of HSM_{50} less than 1 MPa at the SA site in 2018 (Figure 4b, Table S2). The predicted PLC (PLCp) of all species were positive in 2018 and in 2019, except for PHL, which demonstrated neglected PLCp values (Figure 4c,f).

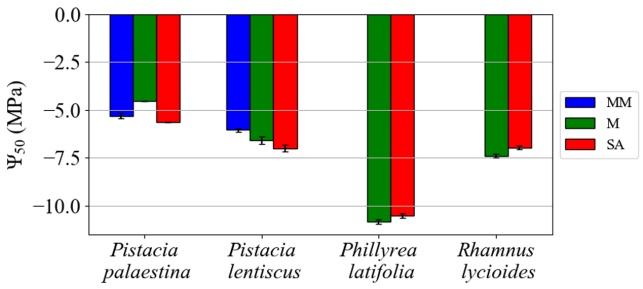

FIGURE 2 Ψ_{50} at the three sites (MM, mesic Mediterranean; M, Mediterranean; SA, semi-arid). *Quercus calliprinos* was not measured due to excessive vessel length. Differences between species were significant, but no significant differences were observed between sites. Error bars indicate standard error (n = 5–7).

3.1.4 | Osmotic potential

Changes in solute potential (Ψ_s) were significant for all the species along the dry season, linearly correlated with the decline in Ψ_{MD}, while a site effect was found only for PL (Figure 5a–e, Tables S6 and S7). Osmotic adjustment, that is, the seasonal decrease in Π_0 differed substantially among species, being large in PHL and QC, minor in RL, negligible in PL and nonexistent in PP (Figure 5f–j, Tables S8–S10). Only QC, PHL and RL had a Ψ_{MD} effect on Π_0. There was a site effect on Π_0 for PHL and PL, while no effect for the interaction of Ψ_{MD} with site was revealed for any of the species (see Table S9). The largest osmotic adjustment was observed for PHL, and ranged from −2 to −5 MPa along the dry season, with similar responses at all sites (Figure 5j). Osmotic adjustment for QC ranged from −2 to −3 MPa during the dry season, mostly at the M and SA sites (Figure 5f).

3.2 | Interspecific variation

A comparison of the interspecific variation between means of Ψ_{PD} among sites using Bartlett's test for homogeneity of variances, resulted in a significant difference (p = 0.026) between sites at the beginning of the dry season. Interspecific variation was more pronounce at the SA site than at the M and MM sites (Table 4).

Species showed different evolution of Ψ_{PD} along the dry season, and reached different values at the end of the season (Figure 3a–e). In each site, the interspecific variation increased during the dry season, however, the increase was significant (p = 0.026) only at the M site (Table 5). Slopes of Ψ_{PD} along the dry season were different between species in each site, while the higher value was that of RL and PHL, followed by PL, PP and QC (see Table S11).

3.3 | The relationships between Ψ_{PD} and Ψ_{MD}

Analysis of the relationships between Ψ_{PD} and Ψ_{MD} at the various sites for each species showed that the slopes at the drier sites (M and SA) were steeper than the slope at the MM site, except for QC and PHL (see Table S12). However, covariance analysis did not show significant differences between the slopes, except for PL (see Table S13). Hydroscape values for all species were larger at the SA site than at the two wetter sites except for PHL (Figure 3f–j, Table S12). Analysis, which includes the data from the various sites for each species, showed that slopes ranged

TABLE 3 Two-factorial ANOVA of the effect of species, site and the interaction between site and species on all measured traits. For all embolism resistance parameters the two-factor analysis was done on four species (PL, PP, PHL and RL) for two sites (M and SA). For the other parameters, analysis was done on four species (QC, PL, PP and PHL) for three sites. Bold *p* values indicate statistically significant result.

Trait	Species	Site	Species*site
Ψ_{50}	$F(3,19) = 84.5056$, **$p = <0.0001$**	$F(1,19) = 0.4501$, $p = 0.508$	$F(3,19) = 1.4025$, $p = 0.2636$
Ψ_{12}	$F(3,19) = 17.4657$, **$p = <0.0001$**	$F(1,19) = 0.0105$, $p = 0.919$	$F(3,19) = 0.6733$, $p = 0.5759$
Ψ_{88}	$F(3,19) = 27.4226$, **$p = <0.0001$**	$F(1,19) = 0.719$, $p = 0.4039$	$F(3,19) = 0.1714$, $p = 0.9148$
Slope	$F(3,15) = 0.6424$, $p = 0.5944$	$F(1,15) = 0.0095$, $p = 0.9229$	$F(3,15) = 0.9251$, $p = 0.442$
Ψ_{min} (2018)	$F(3,75) = 84.7131$, **$p = <0.0001$**	$F(2,75) = 68.5311$, **$p = <0.0001$**	$F(6,75) = 4.9622$, **$p = 0.0003$**
Ψ_{min} (2019)	$F(3,39) = 92.7639$, **$p = <0.0001$**	$F(2,39) = 19.4777$, **$p = <0.0001$**	$F(6,39) = 2.0137$, $p = 0.087$
Leaf $\delta^{13}C$ / WUEi	$F(3,33) = 2.4531$, $p = 0.0806$	$F(2,33) = 22.3469$, **$p = <0.0001$**	$F(6,33) = 1.3517$, $p = 0.2629$
PLCp (2018)	$F(3,75) = 61.1677$, **$p = <0.0001$**	$F(2,75) = 13.0761$, **$p = <0.0001$**	$F(6,75) = 8.4556$, **$p = <0.0001$**
PLCp (2019)	$F(3,39) = 62.9183$, **$p = <0.0001$**	$F(2,39) = 9.6769$, **$p = 0.0004$**	$F(6,39) = 6.3173$, **$p = 0.0001$**
HSM_{12} (2018)	$F(3,75) = 109.954$, **$p = <0.0001$**	$F(2,75) = 57.7828$, **$p = <0.0001$**	$F(6,75) = 10.5175$, **$p = <0.0001$**
HSM_{12} (2019)	$F(3,75) = 110.3402$, **$p = <0.0001$**	$F(2,75) = 48.928$, **$p = <0.0001$**	$F(6,75) = 10.6456$, **$p = <0.0001$**
HSM_{50} (2018)	$F(3,75) = 111.7792$, **$p = <0.0001$**	$F(2,75) = 40.8695$, **$p = <0.0001$**	$F(6,75) = 11.3523$, **$p = <0.0001$**
HSM_{50} (2019)	$F(3,39) = 87.4207$, **$p = <0.0001$**	$F(2,39) = 17.8401$, **$p = <0.0001$**	$F(6,39) = 5.0945$, **$p = 0.0006$**
HSM_{88} (2018)	$F(3,39) = 88.1662$, **$p = <0.0001$**	$F(2,39) = 14.9253$, **$p = <0.0001$**	$F(6,39) = 5.0271$, **$p = 0.0007$**
HSM_{88} (2019)	$F(3,39) = 89.8414$, **$p = <0.0001$**	$F(2,39) = 12.7135$, **$p = <0.0001$**	$F(6,39) = 5.5257$, **$p = 0.0003$**
Ψ_{PD}(Sep_2018)	$F(3,74) = 73.7787$, **$p = <0.0001$**	$F(2,74) = 39.6804$, **$p = <0.0001$**	$F(6,74) = 2.3523$, **$p = 0.0391$**
Ψ_{PD}(May_2018)	$F(3,32) = 17.1726$, **$p = <0.0001$**	$F(2,32) = 85.8451$, **$p = <0.0001$**	$F(6,32) = 21.302$, **$p = <0.0001$**
Ψ_s (June 2019)	$F(3,11) = 10.7141$, **$p = <0.0001$**	$F(2,11) = 0.3355$, $p = 0.7179$	$F(6,11) = 1.8519$, $p = 0.1263$
Π_0 (June 2019)	$F(3,11) = 21.5185$, **$p = <0.0001$**	$F(2,11) = 7.5033$, **$p = 0.0033$**	$F(6,11) = 4.9563$, **$p = 0.0024$**

from 0.83 for QC to 0.68 for RL (see Table S14). For QC and PP, the extrapolated values were several MPa lower than the lowest data points, −8.9 and −8.7 MPa respectively. However, for PHL, RL and PL the lowest points were close to the regression values at equality, −8.7, −7.6 and −7.1 MPa respectively. Hydroscape values were 10.7, 9.15, 7.31, 6.31 and 3.52 MPa^2, for RL, PHL, PL, PP and QC respectively (see Table S14).

3.4 | Species characterization by drought-resistance strategies

The results described above allowed the assessment of drought-resistance strategies for each of the studied species (Figure 6). That was achieved by quantifying tolerance, avoidance and escape strategies, as described in the Material and Methods (see Table S15). Thus, we found that extreme resistance to embolism confers tolerance in PHL, which also uses osmotic adjustment to resist drought. Osmotic adjustment is a major trait in QC, which probably has deep roots to access water, supporting its stomatal opening during drought. PL and RL do not show osmotic adjustment but have intermediate values of resistance to embolism and almost complete stomatal closure in severe drought. PP has relatively low resistance to embolism and no osmotic adjustment, but its continued water uptake along the dry season suggests it has deep roots. RL is known to escape drought by partial leaf defoliation (Gazol et al., 2017).

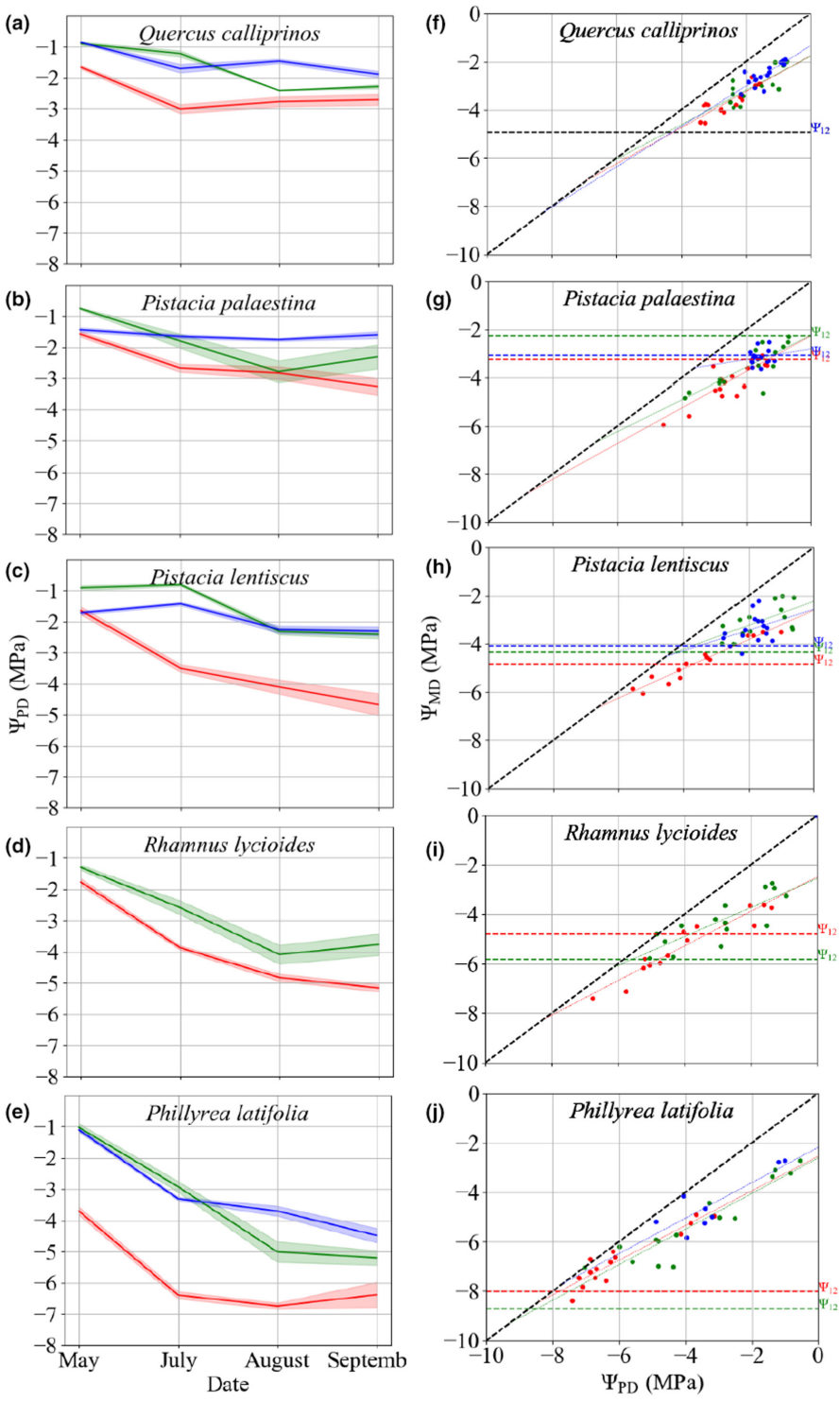

FIGURE 3 Leaf water potential values during the dry season of 2018 at the mesic Mediterranean (blue), Mediterranean (green) and semi-arid (red) study sites. (a–e) Courses of predawn leaf water potential for each species. Line shadow represents standard error. (f–j), Midday water potential (Ψ_{MD}) versus predawn water potential (Ψ_{PD}) for all species during the dry season. Each point on a plot is the average of two twigs. Regression parameters can be found in Table S12. Thick dashed black line represents 1:1 ratio. The thin coloured lines are the regressions of all points of each site from which HS were calculated. Horizontal dashed lines indicate the point of incipient embolism (Ψ_{12}) values for the MM (blue), M (green) and SA (red) sites. Horizontal dashed black line in f indicates the point of incipient embolism based on *Q. coccifera* data (see Section 2). Horizontal dashed blue lines in (i and j) are missing due to insufficient replicates (see Section 2).

4 | DISCUSSION

This study demonstrates differences in drought-related mechanisms among five co-occurring woody species along a climatic gradient. Species differed in xylem resistance to embolism but did not demonstrate plasticity in this trait along the climatic gradient. All species showed a plastic stomatal response, which was demonstrated by leaf water potential. Osmotic potential decreased in all species as a function of water potential; however, substantial osmotic adjustment differences were observed among species.

4.1 | Relating environmental factors to phenotype

The large dataset provided by this study, encompassed three aspects of environmental drought, including site aridity, seasonal

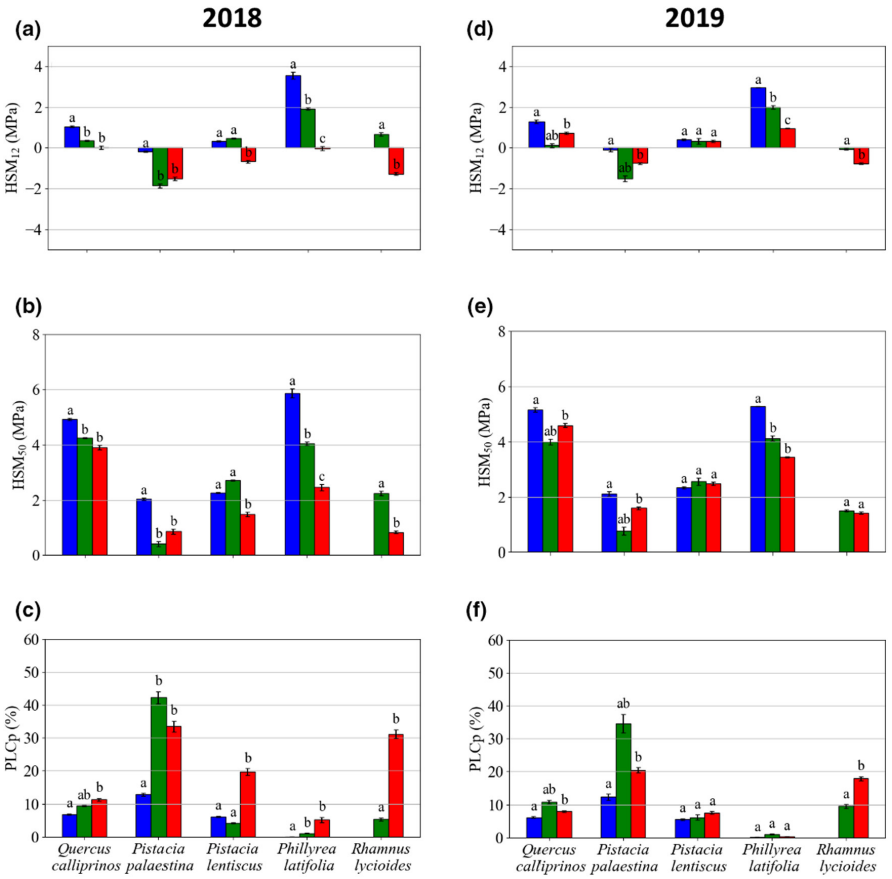

FIGURE 4 HSMs—Hydraulic safety margins (HSM_{12} and HSM_{50}) and PLCp (% of predicted embolism) for all species at the different sites, (a–c) represent 2018 data, (d–f) represent 2019 data. MM, mesic Mediterranean; M, Mediterranean; SA, semi-arid. Different lowercase letters denote significant differences among sites within each species. HSMs of QC are based on the PLC curve of *Q. coccifera* (see Section 2). Error bars indicate standard error ($n = 5$–7).

drought and interannual climate differences. While all site characteristics were less favourable at the SA site than at the two wetter sites, precipitation and VPD differed the most, and actually played major roles in determining the drought intensity of the site. The rainless summer, together with the interannual precipitation differences, further emphasized the stress intensity that the studied species confronted. The SA site differed significantly from the other two sites for most of the traits, suggesting that species were closer to their physiological limits at the dry edge. The latter is in agreement with Feng et al. (2019) and Guo et al. (2020) who emphasized that temporal and spatial variability in the environment is important in determining plant response to drought, as opposed to characterization of species without considering environmental influences.

Our results show interspecific variation in resistance to embolism (Figure 2). However, no intraspecific variation was evident for this trait. A lack of intraspecific variation is in agreement with previous studies that showed similar resistance to embolism in distantly separated populations (Bittencourt et al., 2020; González-Muñoz et al., 2018; Lamy et al., 2014; Li et al., 2018; Lobo et al., 2018; Martínez-Vilalta et al., 2009). However, although the three tested sites differ in climate characteristics, the lack of intraspecific variation might also be due to the continuous geographical distribution of the tested species (see Figure S2), which prevented differentiation between populations due to continuous gene flow. In addition, it is possible that other remote populations, which were not included in the current study, do possess intraspecific variation in resistance to embolism. Several studies have reported intraspecific variation in resistance to embolism in angiosperms. Examples are *Cordia alliodora*, *Artemisia tridentate*, *Fagus sylvatica*, *Populus trichocarpa*, and in Mediterranean and chaparral shrubs (Choat et al., 2007; Jacobsen et al., 2014; Kolb & Sperry, 1999; Pratt et al., 2012; Sparks & Black, 1999; Stojnić et al., 2018; Wortemann et al., 2011).

As opposed to the stability of resistance to embolism, the stomatal response was very plastic as reflected in changes in leaf water potential (Ψ_{PD} and Ψ_{MD}) in response to drought in all species in relation to site aridity, seasonality and interannual climate differences (Figure 3, Table 3). The difference between species in the Ψ_{PD} slope along the season, especially at the SA site (Figure 3, Table S11), suggests species differentiation in the degree of plasticity, where RL and PHL showed the strongest, and QC showed the least plastic response. The interspecific variation in Ψ_{PD} seemed to increase with drought and along the dry season, that is, it was inversely related to aridity (Tables 4 and 5). The HS (see Tables S8 and S9), which showed differences between species, can be used as proxies for stringency of stomatal regulation (Meinzer et al., 2016). Accordingly, QC showed the most stringency of stomatal regulation having the smallest HS value, whereas PHL and RL had the largest HS values and showed the least stringency of stomatal regulation (Figure 3, Tables S12 and S14).

Variations in Ψ_{PD} between species along the dry season may reflect differences in root depth, where Ψ_{PD} of more deeply rooted species, such as QC, appears high with weak plasticity along the

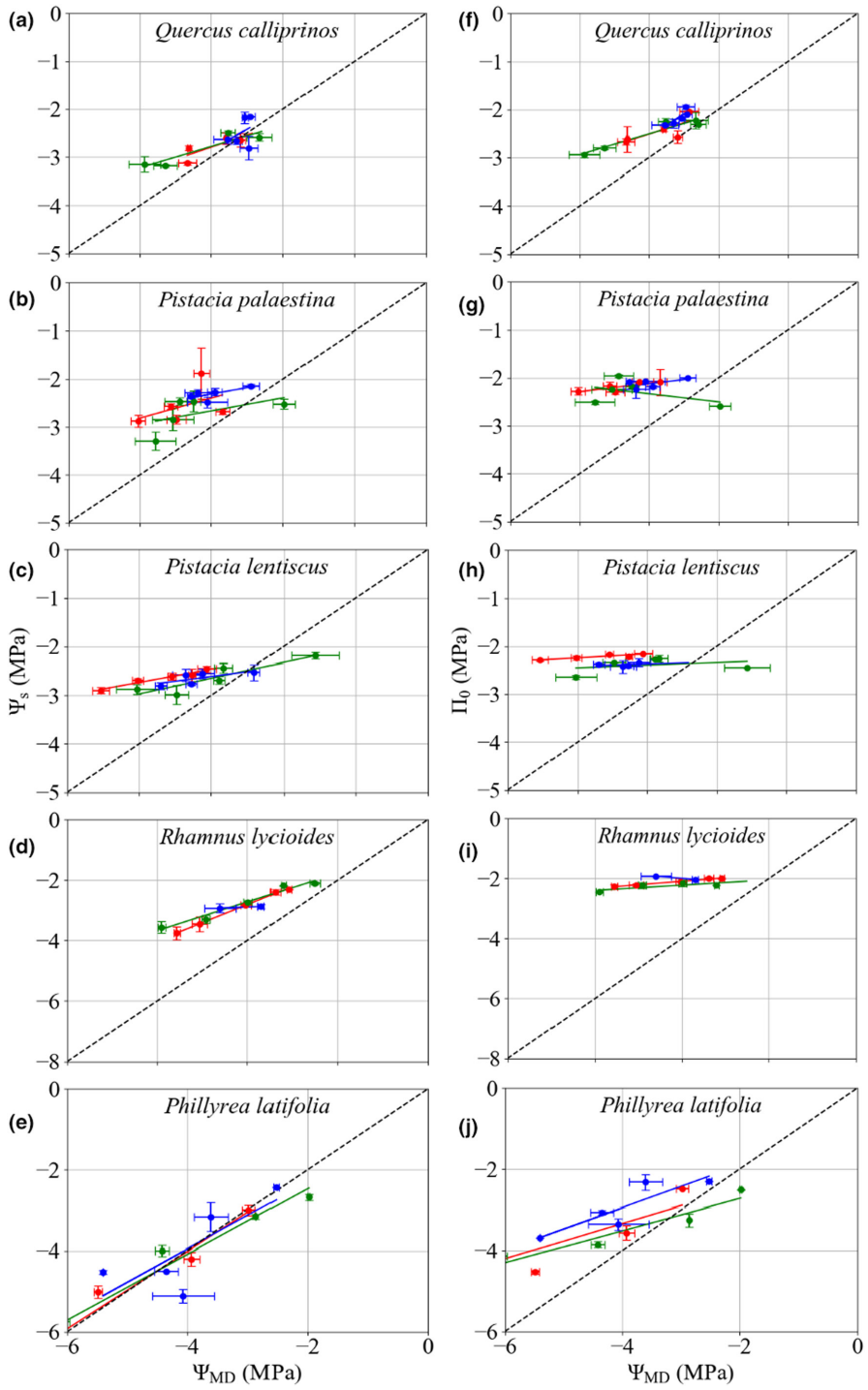

FIGURE 5 Osmotic potential and leaf water potential for all species measured in summer 2019 at the mesic Mediterranean (blue), Mediterranean (green) and semi-arid (red) sites. (a–e) Leaf water potential at midday (Ψ_{MD}) versus native osmotic potential (Ψ_s). (f–j) Ψ_{MD} versus osmotic potential at full turgor (Π_0). Regression parameters for Π_0 can be found in Table S10.

TABLE 4 Bartlett's test for homogeneity of variances for all species per date at the different sites. Bold indicates significant difference.

		Standard deviation				
Parameter	Measurement date	MM	M	SA	χ^2	*p* value
Ψ_{PD}	May 2018	0.374	0.201	0.922	$\chi^2(2) = 3.655$	**0.026**
Ψ_{PD}	July 2018	0.860	0.894	1.474	$\chi^2(2) = 0.389$	0.687
Ψ_{PD}	August 2018	0.998	1.273	1.726	$\chi^2(2) = 1.308$	0.309
Ψ_{PD}	September 2018	1.308	1.284	1.731	$\chi^2(2) = 0.2$	0.819

TABLE 5 Bartlett's test for homogeneity of variances for all species per site at the different dates. Bold indicates significant difference.

Parameter	Site	Standard deviation				χ^2	*p* value
		May	July	August	September		
Ψ_{PD}	SA	0.922	1.474	1.726	1.731	$\chi^2(3) = 0.532$	0.660
Ψ_{PD}	M	0.201	0.894	1.273	1.284	$\chi^2(3) = 3.092$	**0.026**
Ψ_{PD}	MM	0.374	0.860	0.998	1.308	$\chi^2(3) = 1.139$	0.332

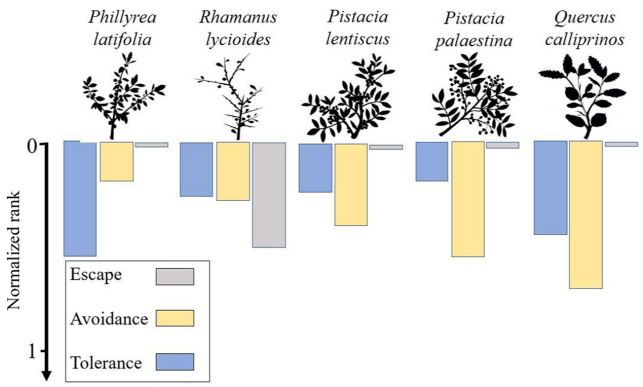

FIGURE 6 A superposition for the three different drought-resistance strategies (tolerance, avoidance and escape) for a species, evaluated as normal parameters (scaled from 0 to 1) derived from measured parameters. Detailed evaluations are presented in Supporting Information Table S15. Drawing by Ilana Stein.

season (Crombie et al., 1988). Roots of 5 m depth have been reported for PP (Jakoby et al., 2020) and QC (Canadell et al., 1996). This is in agreement with Palacio et al. (2017), who demonstrated co-existing species with different root depths sustain niche segregation to share soil water resources. Redtfeldt and Davis (1996) and Rog et al. (2021) also investigated niche segregation in terms of water use patterns. The latter emphasized its importance in increasing forest productivity and carbon sink in semi-arid regions. Our approach to summarize drought-resistance strategies for the different species based on measurements in increasing temporal and local drought suggests current and future niche segregation.

4.2 | The dearth of hydraulic safety margins near the dry edge of species distribution

The Ψ_{50} HSM seemed to change according to annual precipitation as reflected by increasing PLCp in dry 2018 compared to 2019 (Figure 4), especially at the SA site, suggesting that a drought year would have more impact on species vulnerability. This is in agreement with Ziegler et al. (2019), who showed that for tropical trees the Ψ_{50} HSM became narrower, but still positive, in dry years. In the current study, all species (except for QC) crossed the Ψ_{12} threshold (Figure 3f–j), at which point some degree of difference between Ψ_{PD} and Ψ_{MD} remained, suggesting that species maintain some stomatal opening when embolism is low. As drought became more sever, PL, RL and PHL Ψ_{min} at the SA site was similar to the water potential for complete stomatal closure (Ψ_{g_0}), indicating that these plants approached the point of null activity (Figure 3f–j). QC and PP did not seem to reach that point and demonstrated Ψ_{min} that was higher by more than 1 MPa than their water potential for complete stomatal closure Ψ_{g_0}.

Interestingly, PP had a negative Ψ_{12} HSM in all sites in both years (Figure 4), emphasizing the trade-off between hydraulic safety and carbon assimilation in this winter-deciduous species. In addition, results of predicted PLC (PLCp, Figure 4c,f) suggest that all species, except PHL, experienced embolism, which increased with drought intensity. These results suggest that those species approach the limit of hydraulic capacity at the site near the dry margins of their distribution. Taking a modelling approach, Benito Garzón et al. (2018) used minimum soil water potential data and HSMs of 44 European woody species and found that negative HSMs explained the mortality of 15 species at the driest margins of their distribution. With respect to PHL, it is not clear what limits its distribution into the dry region (see Figure S2), as its hydraulic structure is not threatened. The low Ψ_{PD} indicates that PHL has a shallow root system (Nardini et al., 2016; Väänänen et al., 2020) that senses the drought early in the dry season, provoking stomatal closure that limits the growth period by the length of the cold-wet season. In addition, it is possible that the strong OA requires energy investment that cannot be maintained in drier sites.

4.3 | Interspecific variation in response to drought

The interspecific variation in Ψ_{PD} increased with aridity and along the dry season (Tables 4 and 5). This difference was supported by the significant effect of the species-by-site interaction on Ψ_{PD} (Table 3). However, the increase in interspecific variation with site aridity appeared statistically significant only at the beginning of the dry season. These results are another way of showing the limitation of dryness on species distribution, as the interspecific differences, as expressed by the standard deviation, are significantly larger in the SA (0.922) than in the M (0.201) and MM (0.374) sites already at the end of the winter. This suggests that the annual precipitation is a limiting factor for species-specific physiological operation.

As all the species in our study suffered from severe drought at the SA site, as manifested in a significant reduction in HSMs, not all showed osmotic adjustment (which is related to TLP), suggesting that this mechanism is species dependent. Osmotic adjustment in

drought has been reported for PHL (Serrano et al., 2005), and is also well known in Olive species, which are related to PHL (*Oleaceae*; Lo Gullo & Salleo, 1988; Sofo et al., 2008). It has also been reported for PL (Álvarez et al., 2018) in response to salinity and in *Quercus* species (Aranda et al., 2020; Delıgö & Bayar, 2018), but not in QC. The low degree of osmotic adjustment in RL and nonexistent osmotic adjustment in PP may also be related to their deciduous nature. It may result from a strategy of allocating fewer resources to the leaf, similar to the findings of Liu et al. (2011), who showed higher capacities for osmotic adjustment in evergreen shrubs than in deciduous species. It is important to note that the other two mechanisms for turgor maintenance, that is, elastic and apoplastic adjustments (Bartlett et al., 2012; Meinzer et al., 2014), were not evaluated in the current study and may play a role in response to drought in the studied species.

5 | CONCLUSIONS

Figure 6 summarizes how each of the co-occurring species in our study combines different drought-resistance strategies to minimize the risk of mortality. The quantification in the figure is an initial attempt (see methods) which might lead to more implicit modelling of the implications of our findings, for example, geographical and climate limits of the species. However, modelling was beyond the scope of the current study.

We show that RL and PP clearly approached the limit of their hydraulic capacity at the site near the dry margins of their distribution. As the hydraulic limit was more pronounced in the drier year, we argue that a slight reduction in precipitation is more likely to put species at the dry margins of their distribution at the risk of mortality. Our study suggests that RL and PP had more than 30% PLCp in the SA. We therefore predict that they will be the first to experience mortality in the near future. We assume that changes in the woody species community structure would further have critical impacts on global biodiversity. Our study emphasizes the urgent need to develop models to predict the likely effects of climate change on woody community structures to assist in developing management and conservation strategies.

AUTHOR CONTRIBUTIONS

Asaf Alon, Rakefet David-Schwartz, Shabtai Cohen, Sylvain Delzon and HC designed the experiments and interpreted the data. AA, RB and VL collected and measured field samples. Asaf Alon and RB performed vulnerability curve measurements. Asaf Alon and IR performed carbon isotope measurements. Asaf Alon analysed all data. Asaf Alon, Shabtai Cohen and RDS cowrote the manuscript with contributions from Sylvain Delzon, Hervé Cochard, UH and TK.

ACKNOWLEDGEMENTS

We acknowledge the Ramat Hanadiv team for their administrative expertise and technical assistance. We thank Rotem Attias, Shai Tamari, Feng-Feng and Junzhou Liu for their help in the fieldwork. We thank Gaëlle Capdeville for assisting in the Cavitron measurements. We gratefully acknowledge the help of Dr. Hillary Voet with the statistical analyses and Dr. Ilana Stein (https://www.shanabagina.com/english) for the artwork in Figure 6. This work was supported by the Ministère des Affaires Etrangères et du Développement International (France) and the Ministry of Science (Israel), under the Research Program 'Maïmonide-Israel' to RDS, SD, SC and HC. We thank the editors and reviewers for their constructive and thoughtful comments.

CONFLICT OF INTEREST STATEMENT

The authors declare that they have no competing interest in the preparation of this manuscript. Tamir Klein is an Associate Editor of Functional Ecology, but took no part in the peer review and decision-making processes for this paper.

DATA AVAILABILITY STATEMENT

The raw data supporting the results of this study are available at the Dryad Digital Repository https://doi.org/10.5061/dryad.1vhhmgqxb (Alon et al., 2023).

ORCID

Uri Hochberg https://orcid.org/0000-0002-7649-7004
Ido Rog https://orcid.org/0000-0002-9120-3617
Tamir Klein https://orcid.org/0000-0002-3882-8845
Sylvain Delzon https://orcid.org/0000-0003-3442-1711
Rakefet David-Schwartz https://orcid.org/0000-0001-5923-8636

REFERENCES

Adams, H. D., Zeppel, M. J. B., Anderegg, W. R. L., Hartmann, H., Landhäusser, S. M., Tissue, D. T., Huxman, T. E., Hudson, P. J., Franz, T. E., Allen, C. D., Anderegg, L. D. L., Barron-Gafford, G. A., Beerling, D. J., Breshears, D. D., Brodribb, T. J., Bugmann, H., Cobb, R. C., Collins, A. D., Dickman, L. T., … McDowell, N. G. (2017). A multi-species synthesis of physiological mechanisms in drought-induced tree mortality. *Nature Ecology and Evolution*, *1*(9), 1285–1291. https://doi.org/10.1038/s41559-017-0248-x

Alon, A., Cohen, S., Burlett, R., Hochberg, U., Lukyanov, V., Rog, I., Klein, T., Cochard, H., Delzon, S., & David-Schwartz, R. (2023). Data from: Acclimation limits for embolism resistance and osmotic adjustment accompany the geographic dry edge of Mediterranean species. *Dryad Digital Repository*. https://doi.org/10.5061/dryad.1vhhmgqxb

Álvarez, S., Rodríguez, P., Broetto, F., & Sánchez-Blanco, M. J. (2018). Long term responses and adaptive strategies of *Pistacia lentiscus* under moderate and severe deficit irrigation and salinity: Osmotic and elastic adjustment, growth, ion uptake and photosynthetic activity. *Agricultural Water Management*, *202*(June 2017), 253–262. https://doi.org/10.1016/j.agwat.2018.01.006

Anderegg, W. R. L. (2015). Spatial and temporal variation in plant hydraulic traits and their relevance for climate change impacts on vegetation. *New Phytologist*, *205*(3), 1008–1014. https://doi.org/10.1111/nph.12907

Anderegg, W. R. L., Klein, T., Bartlett, M., Sack, L., Pellegrini, A. F. A., Choat, B., & Jansen, S. (2016). Meta-analysis reveals that hydraulic traits explain cross-species patterns of drought-induced tree mortality across the globe. *Proceedings of the National Academy of*

Sciences of the United States of America, *113*, 5024–5029. https://doi.org/10.5061/dryad.116j2

Aranda, I., Cadahía, E., & Fernández De Simón, B. (2020). Specific leaf metabolic changes that underlie adjustment of osmotic potential in response to drought by four *Quercus* species. *Tree Physiology*, *41*, 728–743. https://doi.org/10.1093/treephys/tpaa157

Bartlett, M. K., Klein, T., Jansen, S., Choat, B., & Sack, L. (2016). The correlations and sequence of plant stomatal, hydraulic, and wilting responses to drought. *Proceedings of the National Academy of Sciences of the United States of America*, *113*, 13098–13103. https://doi.org/10.1073/pnas.1604088113

Bartlett, M. K., Scoffoni, C., & Sack, L. (2012). The determinants of leaf turgor loss point and prediction of drought tolerance of species and biomes: A global meta-analysis. *Ecology Letters*, *15*(5), 393–405. https://doi.org/10.1111/j.1461-0248.2012.01751.x

Benito Garzón, M., González Muñoz, N., Wigneron, J. P., Moisy, C., Fernández-Manjarrés, J., & Delzon, S. (2018). The legacy of water deficit on populations having experienced negative hydraulic safety margin. *Global Ecology and Biogeography*, *27*(3), 346–356. https://doi.org/10.1111/geb.12701

Bittencourt, P. R. L., Oliveira, R. S., da Costa, A. C. L., Giles, A. L., Coughlin, I., Costa, P. B., Bartholomew, D. C., Ferreira, L. V., Vasconcelos, S. S., Barros, F. V., Junior, J. A. S., Oliveira, A. A. R., Mencuccini, M., Meir, P., & Rowland, L. (2020). Amazonian trees have limited capacity to acclimate plant hydraulic properties in response to long-term drought. *Global Change Biology*, *gcb.15040*, 3569–3584. https://doi.org/10.1111/gcb.15040

Canadell, J., Jackson, R. B., Ehleringer, J. R., Mooney, H. A., Sala, O. E., & Schulze, E. D. (1996). Maximum rooting depth of vegetation types at the global scale. *Oecologia*, *108*(4), 583–595. https://doi.org/10.1007/BF00329030

Cernusak, L. A., Ubierna, N., Winter, K., Holtum, J. A. M., Marshall, J. D., & Farquhar, G. D. (2013). Environmental and physiological determinants of carbon isotope discrimination in terrestrial plants. *New Phytologist*, *200*(4), 950–965. https://doi.org/10.1111/nph.12423

Chirino, E., Bellot, J., & Sánchez, J. R. (2011). Daily sap flow rate as an indicator of drought avoidance mechanisms in five Mediterranean perennial species in semi-arid southeastern Spain. *Trees*, *25*(4), 593–606. https://doi.org/10.1007/s00468-010-0536-4

Choat, B., Jansen, S., Brodribb, T. J., Cochard, H., Delzon, S., Bhaskar, R., Bucci, S. J., Feild, T. S., Gleason, S. M., Hacke, U. G., Jacobsen, A. L., Lens, F., Maherali, H., Martínez-Vilalta, J., Mayr, S., Mencuccini, M., Mitchell, P. J., Nardini, A., Pittermann, J., … Zanne, A. E. (2012). Global convergence in the vulnerability of forests to drought. *Nature*, *491*(7426), 752–755. https://doi.org/10.1038/nature11688

Choat, B., Sack, L., & Holbrook, N. M. (2007). Diversity of hydraulic traits in nine Cordia species growing in tropical forests with contrasting precipitation. *New Phytologist*, *175*(4), 686–698. https://doi.org/10.1111/j.1469-8137.2007.02137.x

Cochard, H., Damour, G., Bodet, C., Tharwat, I., Poirier, M., & Améglio, T. (2005). Evaluation of a new centrifuge technique for rapid generation of xylem vulnerability curves. *Physiologia Plantarum*, *124*(4), 410–418. https://doi.org/10.1111/j.1399-3054.2005.00526.x

Cramer, W., Guiot, J., Fader, M., Garrabou, J., Gattuso, J.-P., Iglesias, A., Lange, M. A., Lionello, P., Llasat, M. C., Paz, S., Peñuelas, J., Snoussi, M., Toreti, A., Tsimplis, M. N., & Xoplaki, E. (2018). Climate change and interconnected risks to sustainable development in the Mediterranean. *Nature Climate Change*, *8*(11), 972–980. https://doi.org/10.1038/s41558-018-0299-2

Creek, D., Lamarque, L. J., Torres-Ruiz, J. M., Parise, C., Burlett, R., Tissue, D. T., & Delzon, S. (2020). Xylem embolism in leaves does not occur with open stomata: Evidence from direct observations using the optical visualization technique. *Journal of Experimental Botany*, *71*(3), 1151–1159. https://doi.org/10.1093/jxb/erz474

Crombie, D. S., Tippett, J. T., & Hill, T. C. (1988). Dawn water potential and root depth of trees and understorey species in South-Western Australia. *Australian Journal of Botany*, *36*(6), 621–631. https://doi.org/10.1071/BT9880621

Danin, A., & Plitmann, U. (1987). Revision of the plant geographical territories of Israel and Sinai. *Plant Systematics and Evolution*, *156*(1–2), 43–53. https://doi.org/10.1007/BF00937200

David-Schwartz, R., Paudel, I., Mizrachi, M., Delzon, S., Cochard, H., Lukyanov, V., Badel, E., Capdeville, G., Shklar, G., & Cohen, S. (2016). Indirect evidence for genetic differentiation in vulnerability to embolism in *Pinus halepensis*. *Frontiers in Plant Science*, *7*, 768. https://doi.org/10.3389/fpls.2016.00768

Delıgö, A., & Bayar, E. (2018). Drought stress responses of seedlings of two oak species (*Quercus cerris* and *Quercus robur*). *Turkish Journal of Agriculture and Forestry*, *42*(2), 114–123. https://doi.org/10.3906/tar-1709-29

Delzon, S. (2015). New insight into leaf drought tolerance. *Functional Ecology*, *29*(10), 1247–1249. https://doi.org/10.1111/1365-2435.12500

Delzon, S., Douthe, C., Sala, A., & Cochard, H. (2010). Mechanism of water-stress induced cavitation in conifers: Bordered pit structure and function support the hypothesis of seal capillary-seeding. *Plant, Cell and Environment*, *33*(12), 2101–2111. https://doi.org/10.1111/j.1365-3040.2010.02208.x

Farquhar, G. D., Ehleringer, J. R., & Hubick, K. T. (1989). Carbon isotope discrimination and photosynthesis. *Annual Review of Plant Physiology and Plant Molecular Biology*, *40*, 503–537. https://doi.org/10.1146/annurev.arplant.40.1.503

Feng, X., Ackerly, D. D., Dawson, T. E., Manzoni, S., McLaughlin, B., Skelton, R. P., Vico, G., Weitz, A. P., & Thompson, S. E. (2019). Beyond isohydricity: The role of environmental variability in determining plant drought responses. *Plant Cell and Environment*, *42*(4), 1104–1111. https://doi.org/10.1111/PCE.13486

Forner, A., Valladares, F., & Aranda, I. (2018). Mediterranean trees coping with severe drought: Avoidance might not be safe. *Environmental and Experimental Botany*, *155*, 529–540. https://doi.org/10.1016/j.envexpbot.2018.08.006

Forner, A., Valladares, F., Bonal, D., Granier, A., Grossiord, C., & Aranda, I. (2018). Extreme droughts affecting Mediterranean tree species' growth and water-use efficiency: The importance of timing. *Tree Physiology*, *38*(8), 1127–1137. https://doi.org/10.1093/treephys/tpy022

García de la Serrana, R., Vilagrosa, A., & Alloza, J. A. (2015). Pine mortality in Southeast Spain after an extreme dry and warm year: Interactions among drought stress, carbohydrates and bark beetle attack. *Trees*, *29*(6), 1791–1804. https://doi.org/10.1007/s00468-015-1261-9

Gazol, A., Sangüesa-Barreda, G., Granda, E., & Camarero, J. J. (2017). Tracking the impact of drought on functionally different woody plants in a Mediterranean scrubland ecosystem. *Plant Ecology*, *218*(8), 1009–1020. https://doi.org/10.1007/s11258-017-0749-3

González-Muñoz, N., Sterck, F., Torres-Ruiz, J. M., Petit, G., Cochard, H., von Arx, G., Lintunen, A., Caldeira, M. C., Capdeville, G., Copini, P., Gebauer, R., Grönlund, L., Hölttä, T., Lobo-do-Vale, R., Peltoniemi, M., Stritih, A., Urban, J., & Delzon, S. (2018). Quantifying in situ phenotypic variability in the hydraulic properties of four tree species across their distribution range in Europe. *PLoS ONE*, *13*(5), e0196075. https://doi.org/10.1371/journal.pone.0196075

Guo, J. S., Hultine, K. R., Koch, G. W., Kropp, H., & Ogle, K. (2020). Temporal shifts in iso/anisohydry revealed from daily observations of plant water potential in a dominant desert shrub. *New Phytologist*, *225*, 713–726. https://doi.org/10.1111/nph.16196

Jacobsen, A. L., Pratt, R. B., Davis, S. D., & Tobin, M. F. (2014). Geographic and seasonal variation in chaparral vulnerability to cavitation. *Madrono*, *61*(4), 317–327. https://doi.org/10.3120/0024-9637-61.4.317

Jakoby, G., Rog, I., Megidish, S., & Klein, T. (2020). Enhanced root exudation of mature broadleaf and conifer trees in a Mediterranean

forest during the dry season. *Tree Physiology*, *40*(11), 1595–1605. https://doi.org/10.1093/treephys/tpaa092

Johnson, D. M., McCulloh, K. A., Meinzer, F. C., Woodruff, D. R., & Eissenstat, D. M. (2011). Hydraulic patterns and safety margins, from stem to stomata, in three eastern US tree species. *Tree Physiology*, *31*(6), 659–668. https://doi.org/10.1093/treephys/tpr050

Klein, T., Shpringer, I., Fikler, B., Elbaz, G., Cohen, S., & Yakir, D. (2013). Relationships between stomatal regulation, water-use, and water-use efficiency of two coexisting key Mediterranean tree species. *Forest Ecology and Management*, *302*, 34–42. https://doi.org/10.1016/J.FORECO.2013.03.044

Kolb, K. J., & Sperry, J. S. (1999). Differences in drought adaptation between subspecies of sagebrush (*Artemisia tridentata*). *Ecology*, *80*(7), 2373–2384. https://doi.org/10.1890/0012-9658(1999)080[2373:DIDABS]2.0.CO;2

Lamy, J. B., Delzon, S., Bouche, P. S., Alia, R., Vendramin, G. G., Cochard, H., & Plomion, C. (2014). Limited genetic variability and phenotypic plasticity detected for cavitation resistance in a Mediterranean pine. *New Phytologist*, *201*(3), 874–886. https://doi.org/10.1111/nph.12556

Larter, M., Brodribb, T. J., Pfautsch, S., Burlett, R., Cochard, H., & Delzon, S. (2015). Extreme aridity pushes trees to their physical limits. *Plant Physiology*, *168*(3), 804–807. https://doi.org/10.1104/pp.15.00223

Larter, M., Pfautsch, S., Domec, J.-C., Trueba, S., Nagalingum, N., & Delzon, S. (2017). Aridity drove the evolution of extreme embolism resistance and the radiation of conifer genus *Callitris*. *New Phytologist*, *215*(1), 97–112. https://doi.org/10.1111/nph.14545

Li, X., Blackman, C. J., Choat, B., Duursma, R. A., Rymer, P. D., Medlyn, B. E., & Tissue, D. T. (2018). Tree hydraulic traits are coordinated and strongly linked to climate-of-origin across a rainfall gradient. *Plant, Cell & Environment*, *41*(3), 646–660. https://doi.org/10.1111/pce.13129

Liu, C., Liu, Y., Guo, K., Fan, D., Li, G., Zheng, Y., Yu, L., & Yang, R. (2011). Effect of drought on pigments, osmotic adjustment and antioxidant enzymes in six woody plant species in karst habitats of southwestern China. *Environmental and Experimental Botany*, *71*(2), 174–183. https://doi.org/10.1016/j.envexpbot.2010.11.012

Lo Gullo, M. A., & Salleo, S. (1988). Different strategies of drought resistance in three Mediterranean sclerophyllous trees growing in the same environmental conditions. *New Phytologist*, *108*(3), 267–276. https://doi.org/10.1111/j.1469-8137.1988.tb04162.x

Lobo, A., Torres-Ruiz, J. M., Burlett, R., Lemaire, C., Parise, C., Francioni, C., Truffaut, L., Tomášková, I., Hansen, J. K., Kjær, E. D., Kremer, A., & Delzon, S. (2018). Assessing inter- and intraspecific variability of xylem vulnerability to embolism in oaks. *Forest Ecology and Management*, *424*, 53–61. https://doi.org/10.1016/j.foreco.2018.04.031

Maherali, H., Pockman, W. T., & Jackson, R. B. (2004). Adaptive variation in the vulnerability of woody plants to xylem cavitation. *Ecology*, *85*(8), 2184–2199. https://doi.org/10.1890/02-0538

Martínez-Vilalta, J., Cochard, H., Mencuccini, M., Sterck, F., Herrero, A., Korhonen, J. F. J., Llorens, P., Nikinmaa, E., Nolè, A., Poyatos, R., Ripullone, F., Sass-Klaassen, U., & Zweifel, R. (2009). Hydraulic adjustment of scots pine across Europe. *New Phytologist*, *184*(2), 353–364. https://doi.org/10.1111/j.1469-8137.2009.02954.x

Martin-StPaul, N., Delzon, S., & Cochard, H. (2017). Plant resistance to drought depends on timely stomatal closure. *Ecology Letters*, *20*(11), 1437–1447. https://doi.org/10.1111/ele.12851

Meinzer, F. C., Johnson, D. M., Lachenbruch, B., McCulloh, K. A., & Woodruff, D. R. (2009). Xylem hydraulic safety margins in woody plants: Coordination of stomatal control of xylem tension with hydraulic capacitance. *Functional Ecology*, *23*(5), 922–930. https://doi.org/10.1111/j.1365-2435.2009.01577.x

Meinzer, F. C., Woodruff, D. R., Marias, D. E., Mcculloh, K. A., & Sevanto, S. (2014). Dynamics of leaf water relations components in co-occurring iso- and anisohydric conifer species. *Plant, Cell & Environment*, *37*, 2577–2586. https://doi.org/10.1111/pce.12327

Meinzer, F. C., Woodruff, D. R., Marias, D. E., Smith, D. D., McCulloh, K. A., Howard, A. R., & Magedman, A. L. (2016). Mapping 'hydroscapes' along the iso- to anisohydric continuum of stomatal regulation of plant water status. *Ecology Letters*, *19*, 1343–1352. https://doi.org/10.1111/ele.12670

Mencuccini, M., Minunno, F., Salmon, Y., Martínez-Vilalta, J., & Hölttä, T. (2015). Coordination of physiological traits involved in drought-induced mortality of woody plants. *New Phytologist*, *208*(2), 396–409. https://doi.org/10.1111/nph.13461

Myers, N., Mittermeler, R. A., Mittermeler, C. G., Da Fonseca, G. A. B., & Kent, J. (2000). Biodiversity hotspots for conservation priorities. *Nature*, *403*(6772), 853–858. https://doi.org/10.1038/35002501

Nardini, A., Casolo, V., Dal Borgo, A., Savi, T., Stenni, B., Bertoncin, P., Zini, L., & McDowell, N. G. (2016). Rooting depth, water relations and non-structural carbohydrate dynamics in three woody angiosperms differentially affected by an extreme summer drought. *Plant, Cell & Environment*, *39*(3), 618–627. https://doi.org/10.1111/pce.12646

Nemera, D. B., Bar-Tal, A., Levy, G. J., Lukyanov, V., Tarchitzky, J., Paudel, I., & Cohen, S. (2020). Mitigating negative effects of long-term treated wastewater application via soil and irrigation manipulations: Sap flow and water relations of avocado trees (*Persea americana* mill.). *Agricultural Water Management*, *237*, 106178. https://doi.org/10.1016/j.agwat.2020.106178

Palacio, S., Montserrat-Martí, G., & Ferrio, J. P. (2017). Water use segregation among plants with contrasting root depth and distribution along gypsum hills. *Journal of Vegetation Science*, *28*(6), 1107–1117. https://doi.org/10.1111/jvs.12570

Pammenter, N. W., & Van der Willigen, C. (1998). A mathematical and statistical analysis of the curves illustrating vulnerability of xylem to cavitation. *Tree Physiology*, *18*, 589–593. https://doi.org/10.1093/treephys/18.8-9.589

Pratt, R. B., Jacobsen, A. L., Golgotiu, K. A., Sperry, J. S., Ewers, F. W., & Davis, S. D. (2007). Life history type and water stress tolerance in nine California chaparral species (Rhamnaceae). *Ecological Monographs*, *77*, 239–253. https://doi.org/10.1890/06-0780

Pratt, R. B., Jacobsen, A. L., Jacobs, S. M., & Esler, K. J. (2012). Xylem transport safety and efficiency differ among fynbos shrub life history types and between two sites differing in mean rainfall. *International Journal of Plant Sciences*, *173*(5), 474–483. https://doi.org/10.1086/665267

Redtfeldt, R. A., & Davis, S. D. (1996). Physiological and morphological evidence of niche segregation between two co-occurring species of Adenostoma in California chaparral. *Écoscience*, *3*(3), 290–296. https://doi.org/10.1080/11956860.1996.11682345

Rog, I., Tague, C., Jakoby, G., Megidish, S., Yaakobi, A., Wagner, Y., & Klein, T. (2021). Interspecific soil water partitioning as a driver of increased productivity in a diverse mixed Mediterranean forest. *Journal of Geophysical Research: Biogeosciences*, *126*(9), 1–22. https://doi.org/10.1029/2021JG006382

Serrano, L., Peñuelas, J., Ogaya, R., & Savé, R. (2005). Tissue-water relations of two co-occurring evergreen Mediterranean species in response to seasonal and experimental drought conditions the botanical Society of Japan and Springer-Verlag 2005. *Journal of Plant Research*, *118*, 263–269. https://doi.org/10.1007/s10265-005-0220-8

Skelton, R. P., Dawson, T. E., Thompson, S. E., Shen, Y., Weitz, A. P., & Ackerly, D. (2018). Low vulnerability to xylem embolism in leaves and stems of North American oaks. *Plant Physiology*, *177*(3), 1066–1077. https://doi.org/10.1104/pp.18.00103

Sofo, A., Manfreda, S., Fiorentino, M., Dichio, B., & Xiloyannis, C. (2008). Hydrology and earth system sciences the olive tree: A paradigm for drought tolerance in Mediterranean climates. *Hydrolology &*

Earth System Sciences, *12*, 293–301 www.hydrol-earth-syst-sci.net/12/293/2008/

Sparks, J. P., & Black, R. A. (1999). Regulation of water loss in populations of *Populus trichocarpa*: The role of stomatal control in preventing xylem cavitation. *Tree Physiology*, *19*(7), 453–459. https://doi.org/10.1093/TREEPHYS/19.7.453

Spinoni, J., Vogt, J. V., Naumann, G., Barbosa, P., & Dosio, A. (2018). Will drought events become more frequent and severe in Europe? *International Journal of Climatology*, *38*(4), 1718–1736. https://doi.org/10.1002/joc.5291

Stojnić, S., Suchocka, M., Benito-Garzón, M., Torres-Ruiz, J. M., Cochard, H., Bolte, A., Cocozza, C., Cvjetković, B., de Luis, M., Martinez-Vilalta, J., Ræbild, A., Tognetti, R., & Delzon, S. (2018). Variation in xylem vulnerability to embolism in European beech from geographically marginal populations. *Tree Physiology*, *38*(2), 173–185. https://doi.org/10.1093/TREEPHYS/TPX128

Tielbörger, K., Bilton, M. C., Metz, J., Kigel, J., Holzapfel, C., Lebrija-Trejos, E., Konsens, I., Parag, H. A., & Sternberg, M. (2014). Middle-eastern plant communities tolerate 9 years of drought in a multi-site climate manipulation experiment. *Nature Communications*, *5*, 5102. https://doi.org/10.1038/ncomms6102

Toumi, L., & Lumaret, R. (2010). Genetic variation and evolutionary history of holly oak: A circum-Mediterranean species-complex [*Quercus coccifera* L./*Q. calliprinos* (Webb) Holmboe, Fagaceae]. *Plant Systematics and Evolution*, *290*(1), 159–171. https://doi.org/10.1007/s00606-010-0358-2

Trumbore, S., Brando, P., & Hartmann, H. (2015). Forest health and global change. *Science*, *349*(6250), 814–818. https://doi.org/10.1126/science.aac6759

Turner, N. C. (2017). Turgor maintenance by osmotic adjustment, an adaptive mechanism for coping with plant water deficits. *Plant, Cell & Environment*, *40*, 1–3 https://onlinelibrary.wiley.com/doi/abs/10.1111/pce.12839

Turner, N. C. (2018). Turgor maintenance by osmotic adjustment: 40 years of progress. *Journal of Experimental Botany*, *69*, 3223–3233. https://doi.org/10.1093/jxb/ery181

Tyree, M. T., & Sperry, J. S. (1989). Vulnerability of xylem to cavitation and embolism. *Annual Review of Plant Physiology and Plant Molecular Biology*, *40*(1), 19–36. https://doi.org/10.1146/annurev.pp.40.060189.000315

Tyree, M. T., & Zimmermann, M. H. (1983). *Xylem structure and the ascent of sap*. Springer-Verlag.

Väänänen, P. J., Osem, Y., Cohen, S., & Grünzweig, J. M. (2020). Differential drought resistance strategies of co-existing woodland species enduring the long rainless eastern Mediterranean summer. *Tree Physiology*, *4*, 305–320. https://doi.org/10.1093/treephys/tpz130

Volaire, F. (2018). A unified framework of plant adaptive strategies to drought: Crossing scales and disciplines. *Global Change Biology*, *24*(7), 2929–2938. https://doi.org/10.1111/gcb.14062

Wortemann, R., Herbette, S., Barigah, T. S., Fumanal, B., Alia, R., Ducousso, A., Gomory, D., Roeckel-Drevet, P., & Cochard, H. (2011). Genotypic variability and phenotypic plasticity of cavitation resistance in *Fagus sylvatica* L. across Europe. *Tree Physiology*, *31*(11), 1175–1182. https://doi.org/10.1093/treephys/tpr101

Xu, C., McDowell, N. G., Fisher, R. A., Wei, L., Sevanto, S., Christoffersen, B. O., Weng, E., & Middleton, R. S. (2019). Increasing impacts of extreme droughts on vegetation productivity under climate change. *Nature Climate Change*, *9*(12), 948–953. https://doi.org/10.1038/s41558-019-0630-6

Zar, H. J. (1984). *Multisample hypotheses: The analysis of variance. Biostatistical analysis* (p. 718). Prentice-Hall, Inc.

Ziegler, C., Coste, S., Stahl, C., Delzon, S., Levionnois, S., Cazal, J., Cochard, H., Esquivel-Muelbert, A., Goret, J. Y., Heuret, P., Jaouen, G., Santiago, L. S., & Bonal, D. (2019). Large hydraulic safety margins protect Neotropical canopy rainforest tree species against hydraulic failure during drought. *Annals of Forest Science*, *76*(4), 1–18. https://doi.org/10.1007/s13595-019-0905-0

SUPPORTING INFORMATION

Additional supporting information can be found online in the Supporting Information section at the end of this article.

Figure S1. Leaf δ13C and the derived WUEi of five species at the study sites at the end of the dry season.

Figure S2. Distribution maps of the studied species in Israel.

Figure S3. Per cent loss of conductivity (PLC) curves obtained by the Cavitron method.

Table S1. δ13C ANOVA analysis between species per site per measurement date.

Table S2. Ψ_{50}, Ψ_{12}, Ψ_{88}, Ψ_{min} and safety margins measured for the different species at the different sites in summer of 2018 and 2019.

Table S3. Ψ_{PD} ANOVA analysis between sites per species per measurement date.

Table S4. Ψ_{PD} ANOVA analysis between species per site per measurement date.

Table S5. Ψ_{MD} ANOVA analysis between species per site per measurement date.

Table S6. Summary of covariance analysis testing influence of Ψ_{MD}, species and their interaction on Ψ_S.

Table S7. Summary of covariance analysis testing influence of Ψ_{MD}, site and Ψ_{MD} X site on Ψ_S.

Table S8. Summary of covariance analysis testing influence of Ψ_{MD}, species and their interaction on Π_0.

Table S9. Summary of covariance analysis testing influence of Ψ_{MD}, site and Ψ_{MD} X site on Π_0.

Table S10. Parameters correspond to Ψ_{MD} versus osmotic potential at full turgor (Π_0), in all species at all sites.

Table S11. Parameters correspond to Ψ_{PD} slopes analysis in all species at all sites.

Table S12. Parameters for the linear regression of Ψ_{MD} versus Ψ_{PD} for the different species at the different sites.

Table S13. Summary of covariance analysis testing influence of Ψ_{PD}, site and Ψ_{PD} X site on Ψ_{MD}.

Table S14. Parameters for the linear regression of Ψ_{MD} versus Ψ_{PD} for the different species.

Table S15. Summary of normalized drought strategies.

How to cite this article: Alon, A., Cohen, S., Burlett, R., Hochberg, U., Lukyanov, V., Rog, I., Klein, T., Cochard, H., Delzon, S., & David-Schwartz, R. (2023). Acclimation limits for embolism resistance and osmotic adjustment accompany the geographical dry edge of Mediterranean species. *Functional Ecology*, *37*, 1421–1435. https://doi.org/10.1111/1365-2435.14289